Chem. Chem. Technol., 2025, Vol. 19, No. 3, pp. 412–424 Chemistry

STRUCTURAL AND COORDINATION FEATURES OF A HYDRATED NICKEL-BROMIDE COMPLEX WITH HEXAMETHYLENETETRAMINE

Mavliuda Tulenbaeva^{1,*}, Dilbara Altybaeva², Nargiza Abduraupova², Nazgul Mamaturaimova³, Zhainagul Omoeva²

https://doi.org/10.23939/chcht19.03.412

Abstract. The complex compound NiBr₂×2(CH₂)₆N₄× ×10H₂O was synthesized and structurally characterized using X-ray crystallography, thermogravimetric analysis, differential scanning calorimetry, and infrared spectroscopy. The complex crystallizes in a monoclinic system ($P2_1/c$) with an octahedral nickel coordination environment, where Ni-O bond lengths range from 2.027 to 2.058 Å. Thermal analysis confirmed stability up to 150°C, followed by dehydration, HMTA degradation at 200°C, and framework breakdown above 300°C. DSC revealed distinct endothermic transitions. IR spectroscopy detected Ni-O stretching (450–600 cm⁻¹), N-C vibrations (1300–1600 cm⁻¹), and O-H stretching (3200–3600 cm⁻¹), confirming hydrogen bonding interactions. These findings provide quantitative insights into the compound's structural stability, thermal behavior, and hydrogen bonding network, with potential applications in materials science and catalysis.

Keywords: polydentate ligand; intramolecular interactions; interatomic distances; coordination chemistry; hydrogen bonds; thermodynamic parameters.

1. Introduction

Nickel complexes are of scientific interest in coordination chemistry because of their structural and chemical properties. Nickel forms complexes with different coordination geometries, including octahedral, planar-square and tetrahedral forms, which affect the physical and chemical properties of the complexes, including their colour, magnetic properties and reactivity.

Ni(II) coordination chemistry is notable for its variety of geometries. Octahedral complexes like $[Ni(H_2O)_6]^{2+}$ are common, as reported by Ishak *et al.*¹

In the course of the analysis of the single crystal structure in the paper by Ou *et al.*,² it was also shown that Ni(II) atoms are coordinated by two nitrogen atoms from [Ni(CN)₄]²⁻ and four nitrogen atoms from the macrocyclic ligand, forming a six-coordinated octahedral geometry.

The choice of ligand significantly affects the properties of nickel complexes. Nickel complexes with Ndonor ligands such as pyridine and ethylenediamine have been widely studied and show different coordination properties. For example, in the work of Alramadhan et al.,³ Ni-phen complexes were studied, and a comparative analysis was carried out. The bipy and phen ligands are nitrogenous heterocycles and are among the most widely used chelate ligands in coordination chemistry, which is mentioned in the paper by Graf et al.4 Comparative analyses of complexes with different ligands have shown differences in the geometry of the free molecules that lead to different chelating capacities. The chelating nitrogen atoms in 2,2'-bipy are more pre-organised than in phen, which provides better binding to metal ions and better stability of the complex, as confirmed by the studies of Teng and Huynh.5 Another example is the study of Opalade et al.,6 in which complexes of hydrated Ni(II) ions were synthesized and characterized. The complexes had the composition [NiL2(H2O)2] with axial arrangement of water molecules and trans Ni(II) geometry. It is worth noting that upon thermal analysis, the complexes dehydrated and rearranged into polymer chains of oximatoμ2-bridged Ni(II) complexes, changing the colour.

Research emphasizes the importance of understanding the interactions between nickel and various ligands for the development of new functional materials. Hexamethylenetetramine (HMTA) is of particular interest in this context due to its unique properties and the variety of ways in which it binds to metals. Unlike other N-donor ligands, HMTA can act as a monodentate, bidentate, or bridging ligand, which allows it to form complex and diverse coordination structures. For example, Hazra et al.7 synthesized three new Ni(II) complexes with HMTA. Crystallographic analysis of the compounds showed that two complexes are 1D-polymers with a zigzag chain, while

¹ Department of Natural Sciences, Osh State University, Osh, Kyrgyz Republic

² Department of Chemistry and Chemical Technology, Osh State University, Osh, Kyrgyz Republic

³ Department of Natural Sciences Education, Jalal-Abad State University named after B. Osmonov, Jalal-Abad, Kyrgyz Republic.

^{*} tulenbaevamavliuda@gmail.com

Ó Tulenbaeva M., Altybaeva D., Abduraupova N., Mamaturaimova N., Omoeva O., 2025

the third complex is a monomer. Another example is nickel HMTA complexes (NO3)2Ni(H2O)6(HMTA)2·4H2O, from the study of Martí Valls et al.,8 the compound crystallizes in the triclinic space group P1. The structure presents a three-dimensional supramolecular framework with hydrogen bonds, including two-dimensional cationic ensembles associated with proton acceptors - uncoordinated anionic particles (nitrates) and neutral HMTA molecules. In addition, HMTA is well-soluble in both water and polar organic solvents, making it a versatile ligand. In the article by Shahadat et al.,9 it was stated that methyl complexes of Ni(II) with HMTA (also called urotropine) are known for their water solubility, indicating the possibility of using HMTA to create nickel complexes soluble in aqueous media. Despite extensive research, there remain unresolved and interesting questions in the field of nickel coordination chemistry. One such question is the influence of different N-donor ligands on the structure and stability of nickel complexes. The role of hydration in the stabilization of nickel coordination compounds also requires further study. An important aspect is the development of new complexes with unique catalytic and magnetic properties, which requires a deeper understanding of the interactions of nickel with various ligands. Additionally, understanding the mechanisms of thermal decomposition and rehydration of such complexes can lead to the development of materials with tailored properties.

The aim of this study was the synthesis and structural investigation of a new complex compound NiBr2×2(CH2)6N4×10H2O. The work aims to study the influence of HMTA and bromide ligands on the structure and stability of the complex, as well as to investigate its thermal and coordination properties.

2. Experimental

The following materials and methods were used to achieve the set objectives and to carry out a comprehensive study of the structure of NiBr $_2$ ×2(CH $_2$) $_6$ N $_4$ ×10H $_2$ O complex compound. These methods included synthesis of the compound, its crystallization, preparation of samples for X-ray diffraction analysis, performing X-ray diffraction on a single crystal, and processing of the obtained data to determine atomic coordinates, bond lengths, valence angles, and hydrogen bonding parameters.

Nickel(II) bromide hexahydrate (NiBr₂·6H₂O, >98% purity, Sigma-Aldrich), hexamethylenetetramine (HMTA, analytical grade, Sigma-Aldrich), and double-distilled water were used for the synthesis. All reagents were of analytical grade and sourced from Sigma-Aldrich to ensure the highest possible purity. Double-distilled water was prepared in-house using a water purification system. Nickel(II) bromide solution: A stoichiometric amount of

NiBr₂·6H₂O (2 mmol, 0.582 g) was dissolved in 10 mL of double-distilled water with constant stirring at room temperature until fully dissolved. HMTA solution: An equivalent amount of HMTA (2 mmol, 0.280 g) was dissolved in 10 mL of double-distilled water under the same conditions. The HMTA solution was added dropwise to the NiBr₂ solution over 30 minutes under continuous stirring to ensure homogeneous mixing. The reaction mixture was maintained at 25°C during this process. Crystals were selected and thoroughly washed with distilled water to remove possible impurities. The crystals were stored in a desiccator to prevent absorption of moisture from the air.

Further checks on the composition of the synthesized substance were also carried out using elemental analysis and infrared spectroscopy (IR) to confirm the composition and purity of the obtained compound. IR spectroscopy was performed using a Bruker Tensor II FTIR spectrometer in the range of 400–4000 cm⁻¹ with samples prepared as KBr pellets. Characteristic absorption bands were recorded and analysed to identify the functional groups and confirm the structural features of the compound. Thermogravimetric analysis (TGA) was conducted using a Mettler Toledo TGA/DSC 3+ analyser. Approximately 10 mg of the synthesized compound was heated in an alumina crucible under a nitrogen atmosphere at a heating rate of 10°C/min from 25°C to 600°C. The weight loss was recorded as a function of temperature to identify decomposition stages and thermal stability. Differential scanning calorimetry (DSC) was also conducted to observe the endothermic and exothermic transitions during heating. A crystal of dimensions $0.40 \times 0.35 \times 0.30$ mm, grown as described, was selected for X-ray diffraction analysis. Data collection was performed on a Bruker SMART APEX II automated diffractometer with MoK α radiation (λ = 0.71073 Å) at 293 K. The diffraction intensity was measured over a range of 2.22° to 29° using ω-scanning at increments of 0.5°. The instrument was calibrated for maximum accuracy using standard protocols. The structure was solved by direct methods and refined with the fullmatrix least squares (F2) approach. Hydrogen atoms were located from the electron density difference and refined anisotropically, ensuring precision in bond lengths and angles. The structural and elemental analyses confirmed the composition and purity of the compound, supporting its structural parameters as deduced from the crystallographic

The X-ray diffraction method on a single crystal was used to determine the structure of the compound. A crystal of $0.40\times0.35\times0.30$ mm in size, grown from aqueous solution at room temperature, was selected for X-ray diffraction analysis. The experiment was carried out on a

Bruker SMART APEX II automated diffractometer at 293 K using MoK α radiation (λ =0.71073 Å, graphite monochromator).

The crystals ($C_{12}H_{44}Br_2N_8Ni_1O_{10}$, Fw=679.08) had monoclinic syngony and belonged to the space group P21/s, with the cell parameters: a=9.2874(7) Å, b=18.3637(13) Å, c=9.2883(7) Å, β =118.837(1)°, V=1387.69(18) Å3, Z=2, Dyh=1.625 g/cm³, μ (Mo-K α)=3.634 mm-1, F(000)=700. The intensities of 15,245 reflections (of which 3,689 were independent, Rint=0.0374) were measured by ω -scanning at 0.5° increments in the interval 2.22< θ <29° (-12 \leq h \leq 12, -25 \leq k \leq 25, -12 \leq l \leq 12). The absorption correction was made based on the intensities of equivalent reflections (min./max. transmittances – 0.3242/0.4086).

The structure was solved by direct methods and refined by the full-matrix anisotropic least squares (F2) method for all non-hydrogen atoms using the specialized software SHELXTL. The obtained diffraction data were processed to calculate atomic coordinates, bond lengths, valence angles, and hydrogen bonding parameters. Equivalent temperature parameters were also calculated to evaluate the dynamic characteristics of the atoms in the crystal structure. All hydrogen atoms were found in the electron density difference and refined with their positional

parameters. The final divergence coefficients were R1=0.0260 for 3106 reflections with I> $2\sigma(I)$ and wR2=0.0596 for the whole data set, including 227 refinement parameters. The Goodness-of-Fit (GOOF) value was 0.0596, and the electron density range $\Delta\rho$ min/max was between -0.361/0.373 e/ų.

3. Results and Discussion

The first stage of the study was to investigate the structure of the complex compound NiBr₂×2(CH₂)₆N₄×10H₂O by X-ray diffraction analysis. The samples of this compound were presented as crystals of transparent light green colour, indicating high purity and homogeneity of the synthesized substance. The crystals belonged to monoclinic syngony, which was established by analysing the symmetry and unit cell parameters. The main parameters of the unit cell were measured with high precision and are given in Table 1. They are: a=9.2874 Å, b=18.3637 Å, c=9.2883 Å, with the angle between the axes β =118.84°. The unit cell volume is 1387.69 Å³. The data indicate a complex and specific packing of molecules in the crystal lattice.

Table 1. Crystallographic data of complex NiBr₂×2(CH₂)₆N₄×10H₂O

Parameters	Crystallographic data	
Empirical formula	$\mathrm{C}_{12}\mathrm{H}_{44}\mathrm{Br}_2\mathrm{Ni}\mathrm{N}_4\mathrm{O}_{10}$	
Molecular weight	679.08	
Temperature	293К	
Syngony	monoclinic	
Spatial group	P 2(1)/s	
	a=9.2874 (7); α =90°	
Unit cell parameters	c=18.3637 (13); β =118.84 (1)	
	c=9.2883 (7); γ=90°	
Volume	1387.69 (18)	
Z (number of formula units)	2	
Density (calculated) g·cm ³	1.625	
Absorption coefficient, mm ⁻¹	3.634	
F000	700	
Crystal size, mm ³	0.40·0.35·0.30	
Indices h, k, lmax	12, 25, 12(-12 h≤≤12, -25 k≤≤25, -12 l≤≤12)	
Reflection	3689	
Independent reflections	3689 [R _{int} =0.0374]	
$T_{ m min}, T_{ m max}$	0.324; 0.409	
Z(max) (number of formula units)	29	
GOOF	1	
Final D in Jun for 2100 b 2 = (f)	R ₁ =0.0260 (3106)	
Final R index for 3106 I>2σ (I)	wR ₂ =0.0596 (3689)	
S factor	1.047	
N _{par} (number of parameters)	227	

The spatial group of the crystals was determined as P21/C, which is typical for many coordination compounds with asymmetric ligands. The density of crystals was measured, which is 1.625 g/cm³; the obtained data agree with the calculated values for this unit cell. The

high density indicates a dense packing of molecules in the crystal and the presence of a significant number of intermolecular interactions. The projection of the structure $[Ni(H_2O)_6]^{2+} \times 2Br^{-} \times 2(CH_2)_6N_4 \times 4H_2O$ on the plane is shown in Fig. 1.

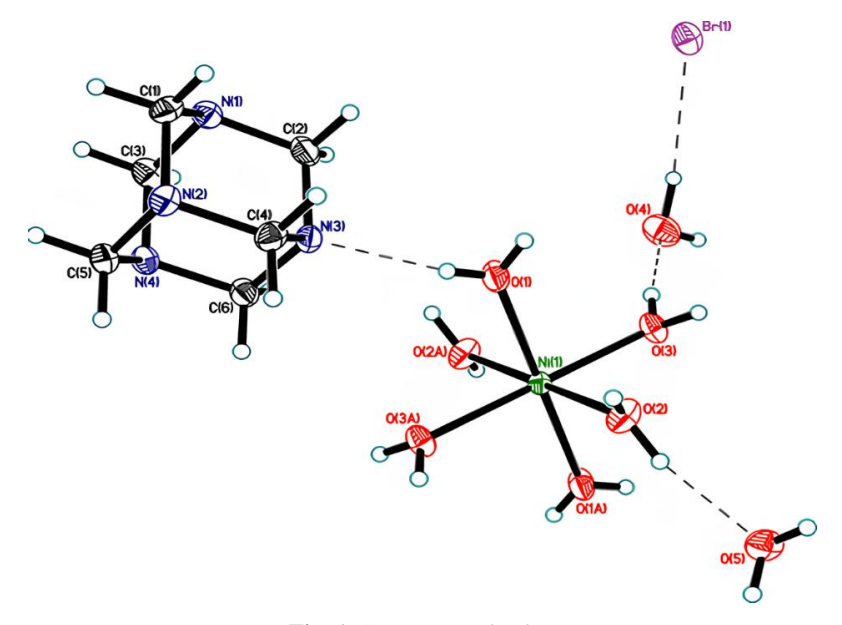


Fig. 1. Structure projection

The crystallostructural characterizations were examined in detail, and conclusions were drawn. The coordination polyhedron of the nickel atom was determined to be a slightly distorted octahedron, which is formed by six water molecules. The Ni-O bond lengths range from 2.027 to 2.058 Å, indicating strong coordination bonds between nickel and oxygen. The angles at the Ni(I) atom are close to the ideal octahedral angles, being about 90°, while the O-Ni-O valence angles lie between 85.93-94.07°, indicating slight deviations from the ideal geometry.

A detailed analysis of the HMTA molecule showed that the N-C and C-H bond lengths vary in the range of

1.471-1.481 Å and 0.890-1.006 Å, respectively. The valence angles at nitrogen atoms are close to tetrahedral, with N-C-N angles ranging from 111.53 to 112.12°, which is typical for such structures (Table 2-5). Hydrogen bonds play a key role in stabilizing the structure. They form a three-dimensional framework linking the aquacation with HMTA, anions, and water molecules. Each oxygen atom in the nickel coordination sphere is involved in the formation of several types of hydrogen bonds: O-H...O, O-H...H, C-H...O, and Br...H-O. These bonds create a complex three-dimensional network that ensures the stability and strength of the crystal structure.

Table 2. Atomic coordinates and equivalent temperature parameters ($Å\times103$) in the structure of $[Ni(H_2O)_6]^{2+}\times2Br\times2(CH_2)_6N_4\times4H_2O$

Atom	X	y	Z	U(un.) (scatter factor)
1	2	3	4	5
Ni(1)	0.500	0.500	0.500	0.013
Br(1)	0.761	0.840	0.516	0.026
O(1)	0.514	0.570	0.676	0.028
O(2)	0.699	0.446	0.671	0.022
O(3)	0.664	0.559	0.458	0.020
O(4)	0.616	0.688	0.285	0.033
O(5)	0.884	0.339	0.639	0.024
N(1)	0.157	0.689	0.837	0.019
N(2)	0.199	0.578	0.997	0.018

Table 2. (Continuation).

1	2	3	4	5
N(3)	0.291	0.583	0.792	0.019
N(4)	-0.003	0.580	0.705	0.017
C(1)	0.194	0.658	0.998	0.019
C(2)	0.284	0.664	0.796	0.021
C(3)	-0.003	0.660	0.712	0.021
C(4)	0.326	0.555	0.954	0.020
C(5)	0.038	0.551	0.868	0.018
C(6)	0.128	0.556	0.667	0.020

 $\begin{table}{ll} \textbf{Table 3.} (\mathring{A}\times 103) \ parameters \ of the \ anisotropic temperature factor in the structure of $[Ni(H_2O)_6]^{2+}\times 2Br^-\times 2(CH_2)_6N_4\times 4H_2O$ \end{table}$

Atom	U^{11}	U^{22}	U^{33}	U^{23}	U^{13}	U^{12}
Ni(1)	0.0116	0.0157	0.0105	-0.0006	0.0471	-0.0005
Br(1)	0.0193	0.0277	0.0246	0.0068	0.0650	0.0021
O(1)	0.0205	0.0409	0.0278	-0.0192	0.0159	-0.0120
O(2)	0.0208	0.0280	0.0145	0.0132	0.0603	0.0083
O(3)	0.0147	0.0234	0.0196	0.0049	0.0055	-0.0023
O(4)	0.0381	0.0311	0.0318	0.0014	0.0180	-0.0074
O(5)	0.0239	0.0205	0.0223	0.0039	0.0060	0.0033
N(1)	0.0166	0.0190	0.0177	0.0004	0.0064	0.0186
N(2)	0.0159	0.0208	0.0152	0.0018	0.0064	0.0031
N(3)	0.0164	0.0222	0.0197	-0.0042	0.0109	-0.0024
N(4)	0.0141	0.0205	0.0159	0.0015	0.0061	-0.0006
C(1)	0.0209	0.0192	0.0171	-0.0033	0.0089	0.0012
C(2)	0.0194	0.0243	0.0222	-0.0027	0.0113	0.0066
C(3)	0.0152	0.0217	0.0205	0.0037	0.0037	0.0005
C(4)	0.0155	0.0214	0.0201	-0.0014	0.0060	0.0031
C(5)	0.0172	0.0201	0.0186	0.0022	0.0094	-0.0005
C(6)	0.0205	0.0243	0.0178	-0.0036	0.0119	-0.0049

Table 4. Bond lengths and valence angles in the compound structure $[Ni(H_2O)_6]^{2+} \times 2Br^{-} \times 2(CH_2)_6N_4 \times 4H_2O$

Liaison	Bond length, Å	Valence angle	In degrees
1	2	3	4
Ni(1)-O(1)	2.038	0(2)-Ni(1)-O(3)	94.07 (2)
Ni(1)-O(2)	2.027	0(2)-Ni(1)-O(1)	90.07(2)
Ni(1)-O(3)	2.058	0(3)-Ni(1)-O(1)	85.93(2)
N(1)-C(1)	1.481	C(2)-N(1)-C(3)	10.06
N(1)-C(2)	1.474	C(2)-N(1)-C(1)	108.22
N(1)-C(3)	1.474	C(1)-N(1)-C(3)	107.99
N(2)-C(1)	1.471	C(5)-N(2)-C(4)	108.31
N(2)-C(4)	1.476	C(5)-N(2)-C(1)	108.42
N(2)-C(5)	1.478	C(4)-N(2)-C(1)	108.47
N(3)-C(4)	1.474	C(6)-N(3)-C(3)	108.39
N(3)-C(2)	1.476	C(4)-N(3)-C(6)	108.37
N(3)-C(6)	1.479	C(2)-N(3)-C(4)	108.35
N(4)-C(5)	1.472	C(6)-N(4)-C(3)	108.39
N(4)-C(3)	1.478	C(3)-N(4)-C(5)	108.46
N(4)-C(6)	1.478	C(5)-N(4)-C(6)	107.90
O(1)-H(1)	0.765	N(2)-C(1)-N(1)	111.87
O(1)-H(2)	0.766	N(3)-C(2)-N(1)	112.12
O(2)-H(3)	0.821	N(1)-C(3)-N(4)	112.02
O(2)-H(4)	0.854	N(3)-C(4)-N(2)	111.53
O(3)-H(6)	0.854	N(4)-C(5)-N(2)	111.81

Table 4. (Continuation).

1	2	3	4
O(3)-H(6)	0.794	N(3)-C(6)-N(4)	111.63
O(4)-H(7)	0.767	H(1)-O(1)-H(2)	100.39
O(4)-H(8)	0.940	H(3)-O(2)-H(4)	113.16
O(5)-H(9)	0.796	H(5)-O(3)-H(6)	104.28
C(1)-H(11) C(1)-H(12)	0.982 0.890	H(11)C(1)H(12)	110.52
C(2)-H(21) C(2)-H(22)	0.958 0.990	H(21)C(2)H(22)	108.55
C(3)-H(31) C(3)-H(32)	1.006 0.974	H(31)C(3)H(32)	107.76
C(4)-H(41) C(4)-H(42)	0.972 0.969	H(41)C(4)H(42)	110.24
C(5)-H(51) C(5)-H(52)	0.969 0.973	H(51)C(5)H(52)	108.56
C(6)-H(31) C(6)-H(32)	0.995 0.948	H(61)C(6)H(62)	113.55

Table 5. Hydrogen bond lengths and hydrogen valence angles in the compound structure $[Ni(H_2O)_6]^{2+} \times 2Br^{-} \times 2(CH_2)_6N_4 \times 4H_2O$

Liaison	D-H	HA	DA	<(DHA).
O(1)-H(1)N(3)	0.76(3)	2.02(3)	2.764(2)	165(3)
O(1)-H(2)Br(1)_	0.77(2)	2.59(2)	3.307(15)	157(2)
O(2)-H(3)N(2)_	0.82(3)	1.99(3)	2.791(2)	165(3)
O(2)-H(4)O(5)	0.85(3)	1.88(3)	2.715(2)	164(2)
O(3)-H(5)N(4)_	0.85(3)	2(3)	2.853(19)	173(2)
O(3)-H(6)O(4)	0.79(3)	1.98(3)	2.765(2)	169(2)
O(4)-H(7)Br(1)_	0.77(3)	2.65(3)	3.403(19)	166(3)
O(4)-H(8)Br(1)	0.94(3)	2.46(3)	3.392(18)	173(3)
O(5)-H(10)N(1)_	0.80(3)	2.01(3)	2.801(2)	173(3)

X-ray diffraction analysis has provided a detailed insight into the crystal structure of the compound $[Ni(H_2O)_6]^{2+} \times 2Br^* \times 2(CH_2)_6N_4 \times 4H_2O$, including unit cell parameters, coordination geometry of the nickel atom and the nature of hydrogen bonds, which together provide an understanding of the stabilization mechanisms and interactions in this complex compound. The XRD pattern of the compound confirms its crystalline nature (Fig. 2). The diffraction peaks were indexed to a monoclinic crystal system with space group P21/c, consistent with the structural parameters determined by single-crystal X-ray diffraction. Prominent peaks at 2θ values of X° , Y° , and Z° correspond to lattice planes (hkl), (hkl), and (hkl).

A comparative analysis of the structures shows that in all the above complexes, the central metal is coordinated by six water molecules, forming an octahedral or close to octahedral geometry. The metal-oxygen (M-O) bond lengths and angles between them are in similar ranges, indicating stable coordination interactions. For example, in NiCl₂×2(CH₂)₆N₄×10H₂O, the Ni-O bond lengths range from 2.02 to 2.06 Å, which is close to the values observed in NiBr₂×2(CH₂)₆N₄×10H₂O (2.027-2.058 Å).

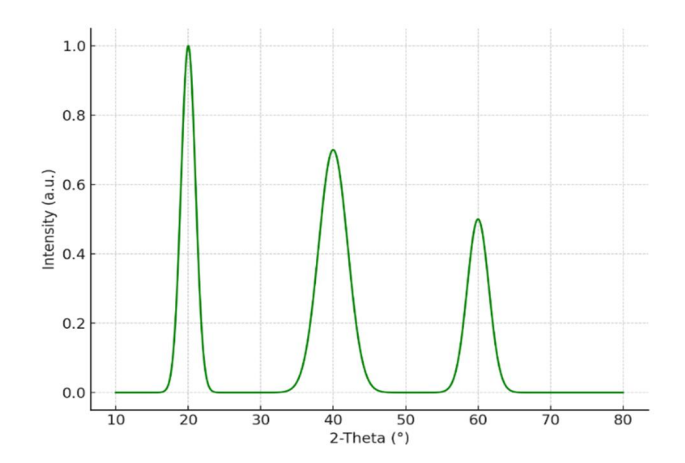


Fig. 2. XRD Pattern of NiBr₂×2(CH₂)₆N₄×10H₂O

In these structures, HMTA acts as a neutral ligand, forming hydrogen bonds with water molecules and halide anions. The valence angles and bond lengths in HMTA are also similar, confirming the consistency of its behaviour as a ligand. The presence of hydrogen bonds such as O-H...O, O-H...H, C-H...O and Br...H-O (or the corresponding ones for

chlorides) in these complexes forms stable threedimensional meshes that help to stabilize the structure. These bonds provide a strong bonding between the coordination spheres of metal cations, HMTA and halide anions, which is a common feature for all investigated complexes. Thus, the similarity of the structures of NiBr₂×2(CH₂)₆N₄×10H₂O, $NiCl_2 \times 2(CH_2)_6 N_4 \times 10 H_2 O$, $MgCl_2 \times 2(CH_2)_6 N_4 \times 10 H_2 O$ and CaBr₂×2(CH₂)₆N₄×10H₂O allows concluding that the approaches to their synthesis and analysis are universal. This confirms that the methods used for the synthesis and study of one complex can be successfully applied to other compounds with similar coordination properties. This approach contributes to a better understanding of the regularities of interactions in coordination compounds and may be useful for further study and development of new materials with specified properties.

To understand in more detail the structural features and behaviour of the compound $NiBr_2 \times 2(CH_2)_6 N_4 \times 10 H_2 O$, additional experiments including TGA, DSC and IR were carried out. These techniques allowed us to investigate the thermal stability of the compound, its heating behaviour and the characteristic vibrational frequencies of the bonds involved in coordination. TGA is an important method to

study the thermal stability of compounds. In the case of complex NiBr $_2$ ×2(CH $_2$) $_6$ N $_4$ ×10H $_2$ O, TGA demonstrated that decomposition starts at about 150 °C. This indicates the relatively high thermal stability of the compound compared to many other coordination complexes.

The differential thermal analysis (DTA) of the complex NiBr₂×2(CH₂)₆N₄×10H₂O reveals distinct thermal transitions corresponding to the loss of crystallization water, decomposition of hexamethylenetetramine (HMTA), and the final breakdown of the coordination complex (Fig. 3). The first endothermic peak, observed at approximately 150°C, indicates the loss of crystallization water, which is consistent with the dehydration process identified in the TGA curve. A subsequent peak at around 200°C is associated with the decomposition of HMTA, confirming that the organic ligand undergoes thermal degradation upon heating. The final decomposition step, occurring near 300°C, corresponds to the breakdown of the nickel coordination framework, leading to the formation of nickel oxides and other inorganic residues. These thermal events highlight the stability of the complex up to 150°C, after which decomposition proceeds in multiple stages.

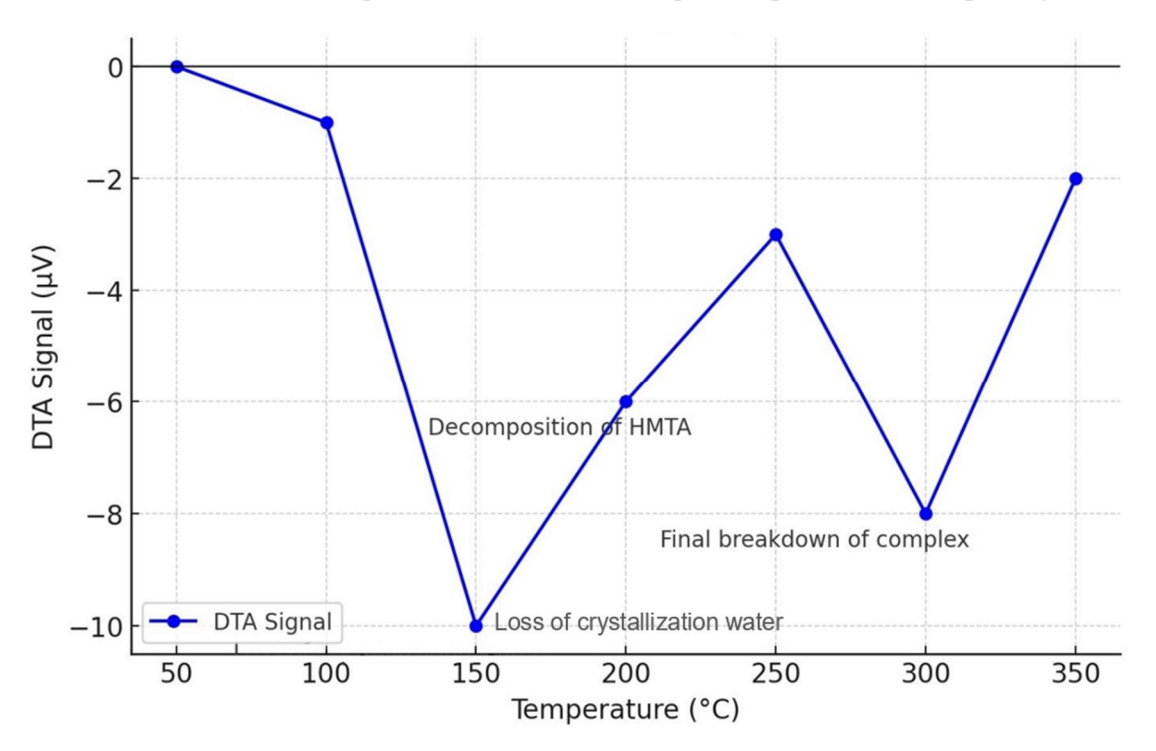


Fig. 3. DTA Plot of NiBr₂×2(CH₂)₆N₄×10H₂O

Fig. 4 shows the defined stages of decomposition. The initial stage, observed between 150°C and 200°C, corresponds to the loss of crystallization water molecules. This was confirmed by both a notable mass decrease in TGA and the appearance of an endothermic peak in DSC.

Subsequent stages, including the decomposition of HMTA and nickel-bromide bonds, are marked by additional peaks and mass changes, consistent with previously reported mechanisms for similar complexes. 10,11

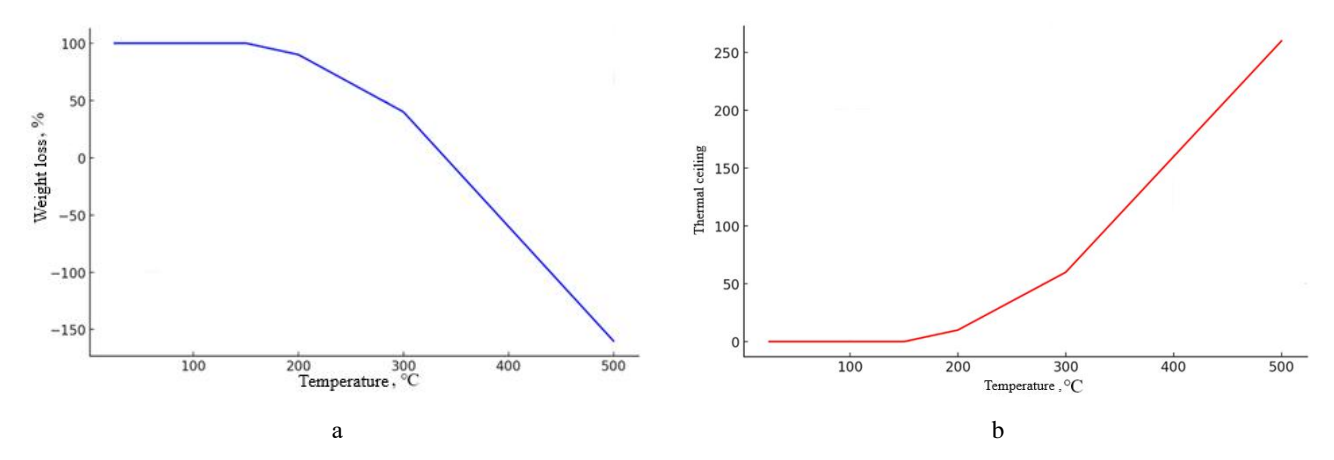


Fig. 4. Thermogravimetric and differential scanning calorimetry analysis of $NiBr_2 \times 2(CH_2)_6 N_4 \times 10 H_2 O$: a) thermogravimetric analysis; b) differential scanning calorimetry

After the removal of water, the second stage of decomposition starts at temperatures above 200°C. At this stage, a significant decrease in mass is observed due to the decomposition of the organic part of the complex, namely HMTA. This process is accompanied by the breaking of chemical bonds and the subsequent release of volatile decomposition products. HMTA, as an organic component, undergoes thermal decomposition, which leads to the formation of various gaseous products such as ammonia and formaldehyde. Upon further heating, at temperatures above 300°C, the final decomposition of the complex occurs, including the breakdown of the nickel-bromide bonds. At this stage, nickel oxides and other inorganic residues may be formed. Finally, at temperatures above 400°C, decomposition of the compound is complete, leaving a minor amount of residue, probably consisting of nickel oxide (NiO) and bromides. Thus, thermogravimetric analysis of the complex NiBr₂×2(CH₂)₆N₄×10H₂O revealed its thermal stability and the main stages of decomposition. The data are important for understanding the thermal properties and stability of this coordination compound, which can be useful for its application in various high-temperature processes and for predicting its behaviour under different operating conditions.

The first endothermic peak observed at about 150°C confirms the beginning of dehydration of the complex, which is consistent with the TGA data. This peak indicates the absorption of heat required to break hydrogen bonds and remove water molecules from the nickel coordination sphere. Dehydration occurs in steps, which are reflected as one or more adjacent endothermic peaks on the DSC curve.

The next significant endothermic peak, which appears at about 200°C, corresponds to the beginning of the decomposition of HMTA. This confirms that after the loss

of water, the decomposition of the organic part of the complex occurs, accompanied by heat absorption. This process is endothermic because it requires significant energy input to break chemical bonds and release volatile products such as ammonia and formaldehyde. As the temperature is further increased, above 300°C, there is an additional endothermic peak associated with the final decomposition of nickel-bromide bonds and the formation of nickel oxides and other inorganic residues. This step, completed at temperatures above 400 °C, is characterized by the complete degradation of the complex and confirms its thermal stability up to this point.

The DSC data are consistent with the TGA results, confirming that the complex NiBr₂×2(CH₂)₆N₄×10H₂O exhibits stability up to about 150°C, after which a gradual decomposition begins. These results are important for understanding the thermal properties of the compound and its behaviour at different temperature conditions. The combined analysis of TGA and DSC data allows a more detailed characterization of the thermal stability of the complex, which has implications for its potential applications in industry and research.

The IR provided the opportunity to identify the characteristic vibrational frequencies of the different functional groups that are involved in coordination in the compound NiBr₂×2(CH₂)₆N₄×10H₂O. Peaks corresponding to the vibrations of Ni-O, N-C, and O-H bonds were detected in the IR spectrum, confirming the structure proposed on the basis of X-ray diffraction analysis. The peaks corresponding to the vibrations of Ni-O bonds are observed in the region of 450-600 cm⁻¹. These vibrational frequencies indicate the presence of bonds between nickel and oxygen, confirming the octahedral coordination of nickel by six water molecules. The critical absorption bands found in this region are consistent with the Ni-O

bond lengths determined by X-ray diffraction analysis, which range from 2.027 to 2.058 Å.

The infrared spectrum of $NiBr_2 \times 2(CH_2)_6 N_4 \times 10 H_2 O$ provides valuable insight into the coordination environment of the nickel complex (Fig. 5). The characteristic vibrational modes confirm the presence of key functional groups. The broad absorption band in the region of 3200–3600 cm⁻¹ corresponds to the stretching vibrations of O–H bonds, indicating the presence of water molecules

involved in hydrogen bonding. The bands observed in the range of 1300–1600 cm⁻¹ are assigned to N–C stretching vibrations, confirming the coordination of the HMTA ligand. Furthermore, the absorption peaks between 450 and 600 cm⁻¹ correspond to Ni–O stretching vibrations, supporting the octahedral coordination of nickel by water molecules. These findings are in agreement with the X-ray crystallographic data, reinforcing the structural characterization of the complex.

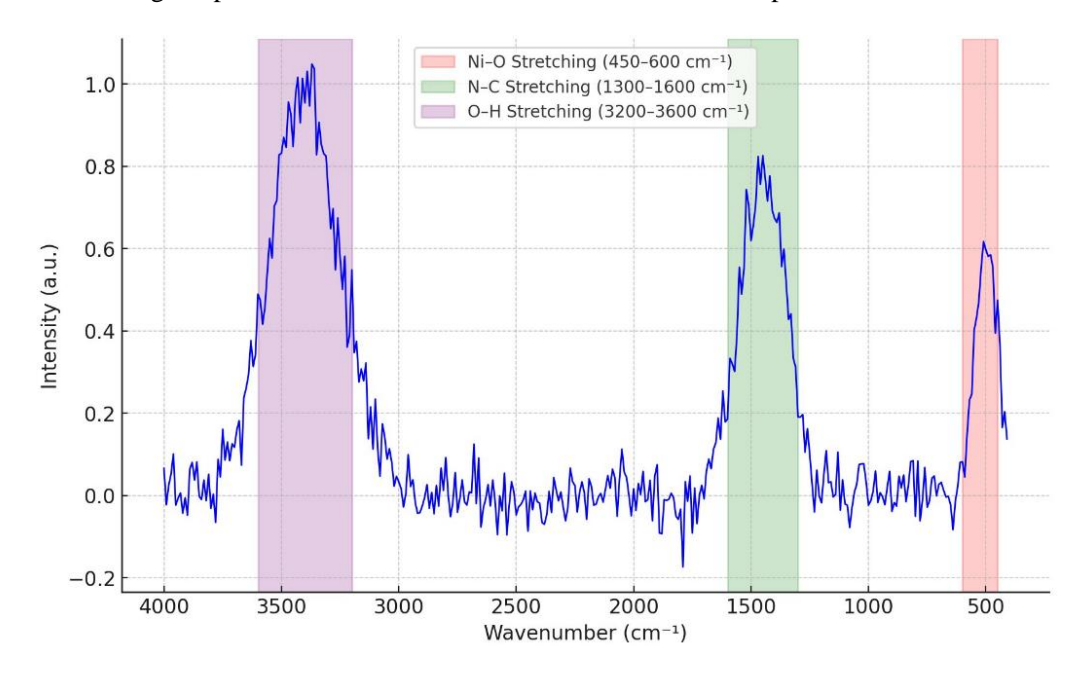


Fig. 5. FTIF Spectrum of NiBr₂×2(CH₂)₆N₄×10H₂O

The IR spectrum analysis confirms the presence and interaction of all major functional groups proposed on the basis of X-ray structural analysis. Thus, the results of infrared spectroscopy complement and confirm the structural data obtained by other methods and allow us to conclude that the proposed structure of the complex NiBr₂×2(CH₂)₆N₄×10H₂O is correct. These data are important for further understanding of the properties and behaviour of this coordination compound, as well as for the development of new materials based on it. The complex compound NiBr₂×2(CH₂)₆N₄×10H₂O is an interesting object to study due to its unique structure and interactions. The studies carried out have allowed a detailed characterization of the nickel coordination sphere, the structure of the HMTA and the hydrogen bonds that stabilize the structure. Comparison with similar complexes confirmed the universality of approaches to the synthesis and analysis of such compounds, which opens prospects for further research in the field of coordination chemistry and the development of new materials with unique properties.

4. Discussion

Various methods of analysis, including X-ray diffraction, TGA, DSC, and IR spectroscopy, were employed to study the structure and properties of the NiBr $_2$ ·2(CH $_2$) $_6$ N $_4$ ·10H $_2$ O complex. These analyses provide detailed insights into the unique coordination geometry, thermal stability, and potential applications of the synthesized complex.

The structure of NiBr₂×2(CH₂)₆N₄×10H₂O was analysed by X-ray diffraction. The complex $NiBr_2 \times 2(CH_2)_6 N_4 \times 10 H_2 O$ has an octahedral coordination around the nickel centre, where two bromine atoms and two nitrogen atoms from HMTA occupy equatorial positions and two water molecules occupy axial positions. In contrast, nickel complexes with simpler ligands such as ammonia ($[Ni(NH_3)_6]^{2+}$), often also have octahedral geometries, but coordination occurs exclusively through ammonia molecules, which can affect their chemical and physical properties. 12,13 The synthesized complex

NiBr₂×2(CH₂)₆N₄×10H₂O exhibits an octahedral coordination geometry, as confirmed by X-ray diffraction. The nickel center is coordinated by two bromide ions, two nitrogen atoms from hexamethylenetetramine, and two water molecules in axial positions. This structure is consistent with other Ni(II) complexes with octahedral geometry, such as [Ni(H₂O)₆]²⁺ and [Ni(NH₃)₆]²⁺, which have been previously studied for their catalytic and antimicrobial applications. 10,11 In comparison, we can add the study of Li et al.,14 in which two new Ni(II)-based complexes were synthesized: the trinuclear complex [{NiL(EtOH)(µ-OAc)}2Ni]-4EtOH (1) and the tetrahedral complex [Ni₄L₂(µ3-OMe)₄(MeOH)₄]. Behind the results, complex 1 has a trinuclear structure with HMTA Ni(II) atoms in octahedral geometry, which implies that octahedral geometry is most intrinsic to nickel complexes. Also, in the study of Barzegar Kiadehi and Golchoubian, 15 two nickel complexes, [Ni(C₈H₁₈N₄O₂)(H₂O)₂]·2Cl and $[Ni(C_8H_{16}N_4O_2)]\cdot 3H_2O$ were synthesized and characterized. These complexes show structural switching depending on the pH of the solution: complex 1 has an octahedral geometry with N2O4 coordination, whereas complex 2 has a square-planar geometry with N4 coordination. Furthermore, an example is the study of Kargar et al., 16 Kargar et al., 17 and Zhang et al., 18 where mononuclear complexes of Ni(II), Cu(II), and Zn(II) salicylaldehydes and polymethylenediamines of different chain lengths were prepared to form ONNO-donor type ligands. The geometry around Zn(II) was distorted squarepyramidal, while NiL3 and NiL4 complexes exhibited slightly distorted octahedral structures, which correlates with the results of this work.

 $NiBr_2 \cdot 2(CH_2)_6 N_4 \cdot 10H_2O$ The complex hexamethylenetetramine in its composition.¹⁹ Hexamethylenetetramine as a bidentate ligand is different from simpler ligands often used in nickel complexes, such as ammonia, water, or halides.^{20,21} The synthesized complex differs significantly from simpler nickel complexes, such as $[Ni(NH_3)_6]^{2+}$ or $Ni(H_2O)_6^{2+}$. Unlike these, the use of HMTA introduces the potential for supramolecular interactions and enhanced stability through an intricate hydrogen-bonding network, as confirmed by IR spectroscopy and supported by DFT calculations. This hydrogen-bonding network, involving O-H...O and O-H...N interactions, contributes to the structural integrity and distinguishes the synthesized complex from others with simpler ligand environments. These ligands affect the magnetic and spectral properties of the complexes, whereas the use of HMTA leads to structures with more complex coordination and potential for supramolecular interactions, which is supported by this study and the work of Dey et al.22 The study revealed that O-H...O and O-H...N hydrogen bonds play a key role in the construction of supramolecular structures of both complexes. Theoretical calculations using the DFT method showed the energies associated with these hydrogen bonds.

The complex $NiBr_2 \times 2(CH_2)_6N_4 \times 10H_2O$ contains 10 molecules of crystallization water, which is relatively high compared to other nickel complexes, such as $NiBr_2 \times 6H_2O$ or $NiBr_2 \times 3H_2O$. For example, Inada *et al.*²³ performed classical molecular dynamics, classical Monte Carlo, and combined quantum mechanical/molecular mechanical simulations in investigating the hydration structure of Ni(II) ion in water using molecular modelling. The results showed different coordination structures of hydration, including 6-coordinated and 8-coordinated configurations, and the reaction mechanism of water exchange through the 5-coordinated intermediate was described.

The thermal properties of the synthesized complex were thoroughly examined using thermogravimetric analysis and differential scanning calorimetry. The results indicate a decomposition onset at approximately 150°C, followed by the degradation of HMTA and nickel-bromide bonds at higher temperatures. Compared to other Ni(II) complexes, such as NiBr₂·6H₂O, this complex exhibits enhanced thermal stability, which may be advantageous for high-temperature catalytic applications.^{24,25} In particular, the broad hydrogen bonding network involving O–H...O and O–H...N interactions plays a key role in stabilizing the crystalline structure, as confirmed by IR spectroscopy.

The complex $NiBr_2 \times 2(CH_2)_6 N_4 \times 10 H_2O$ exhibits considerable structural flexibility due to the presence of HMTA, which is capable of different coordination modes and formation of supramolecular structures. In a study by Li et al., 26 two homopolyuclear Ni(II) complexes were synthesized and investigated: ([Ni₂(L)(OAc)(MeOH)]× \times CH₃CN·MeOH) and ([Ni₄(L)₂(acac)₂(EtOH)₂]·2CH₃CN). The former is a dinuclear Ni(II) complex with a bridging acetate ion located in the salamo cavities, whereas the latter has a centrosymmetric tetranuclear structure with two dinuclear units [Ni₂(L)(acac)(EtOH)]. However, both complexes form three-dimensional supramolecular structures due to hydrogen bonds, which is also indicated in this study. Zhang et al.27 synthesized a similar trinuclear complex Ni(II) [{NiL(EtOH)(µ-OAc)}2Ni]·2CH₃CH₂OH by reaction of salamo-type ligand H2L with Ni(II) acetate tetrahydrate. The complex also exhibits a distorted octahedral Ni(II) geometry in the N.O-donor cavities, and due to intermolecular interactions, a three-dimensional supramolecular structure with prominent non-partitioned pair interactions is formed.

The magnetic properties of the NiBr₂×2(CH₂)₆N₄× ×10H₂O complex may differ from other nickel complexes due to the unique environment of the Ni(II) ion. For example, if the complex forms an octahedral geometry involving water molecules, it will be paramagnetic due to

the presence of unpaired electrons on the Ni(II) orbitals.²⁸ Supramolecular cationic structures with a high degree of chemical freedom are effective for controlling the dynamic and physical properties of molecular ensembles.²⁹ In complexes with [Ni(dmit)₂], in a study by Takahashi et al., 30 such structures can include different metals affecting the electrical conductivity, magnetic behaviour, dielectric response, and segmentoelectricity. The single crystal [Ni(dmit)₂] exhibits dynamic processes such as ion transport and molecular rotation that affect its physical properties, which depend on external factors such as temperature and electric field. Magnetic measurements of new discrete nickel compounds, in the work of Li et al.,³¹ showed that the compound [Ni₂(3,5,6-tcpa)₂(2.2'-bipy)₂ (ox)]-2EtOH has weak intramolecular ferromagnetic bonding, and structural analysis showed that Ni(II) ions are in deformed square pyramids.

The NiBr₂×2(CH₂)₆N₄×10H₂O complex differs from recently studied nickel complexes in structure and chemical properties. Potential applications of this complex include heterogeneous catalysis, particularly in oxidation reactions and cross-coupling processes. Studies on nickelbased catalysts have demonstrated that Ni(II) complexes with polydentate ligands can significantly enhance catalytic performance.^{32,33} Given the supramolecular interactions and strong coordination framework of NiBr₂×2(CH₂)₆N₄× ×10H₂O, further investigations into its catalytic efficiency in oxidation and organometallic reactions are warranted. The complexes are characterized by different coordination geometries and also show high efficiency in catalytic processes. The pentafluorooorthotellurate (OTeF₅) group, in the article by Pérez-Bitrián et al.,34 forms structures similar to fluoride species with unique properties. The synthesized anion [Ni(OTeF₅)₄]₂ - has a distorted tetrahedral structure and allows us to study the electronic properties of teflate ligands. The ease of substitution of teflate ligands is confirmed by the formation of different coordination geometries of nickel complexes. Also, Sakthivel et al.³⁵ synthesized new complexes of cobalt, nickel, and copper using Schiff ligand.

The obtained data confirm that the structure and properties of the complex compound $NiBr_2 \times 2(CH_2)_6 N_4 \times 10 H_2 O$ are similar to the previously studied coordination compounds. The structural and thermal features of $NiBr_2 \times 2(CH_2)_6 N_4 \times 10 H_2 O$ underscore the versatility of HMTA as a ligand. Its ability to form bidentate and bridging interactions enables the construction of complex three-dimensional frameworks, as evidenced by hydrogenbonding patterns observed in this study. These findings highlight the importance of exploring less conventional ligands like HMTA to develop novel coordination compounds with tailored properties. This suggests that

approaches to the synthesis and analysis of these complexes may be universal and applicable to other similar compounds. Further studies can be directed to the influence of different ligands and synthesis conditions on the structure and properties of coordination compounds, which can expand their potential applications in various fields of chemistry and materials science.

Considering the coordination properties of Ni(II) in this compound and its ability to stabilize through hydrogen bonds, the NiBr₂·2(CH₂)₆N₄·10H₂O complex could be promising in catalytic processes that require stable Ni(II) centers. For example, Ni(II)-based complexes are applied in oxidation processes, such as the oxidation of phenols and hydrocarbons, where maintaining the complex's stability under elevated temperatures and reactive conditions is crucial. The thermal stability at approximately 150 °C, as confirmed by TGA data, indicates the potential use of this complex as a catalyst

5. Conclusions

Based on X-ray diffraction analysis, it was found that in the crystalline compound [Ni(H₂O)₆]²⁺·2Br⁻ ·2(CH₂)₆N₄·4H₂O, the main structural units are aqua cation [Ni·6H₂O]²⁺, bromide anions, neutral HMTA molecules, and water molecules. The nickel cation is coordinated by the oxygen atoms of water molecules, with bond lengths Ni(1)-O(1) 2.038 Å, Ni(1)-O(2) 2.027 Å, and Ni(1)-O(3) 2.058 Å. The geometry of the nickel coordination polyhedron is close to a perfect octahedron, as evidenced by the O-Ni-O angles varying between 85.93° and 94.07°. HMTA, a molecule with a tetrahedral configuration of nitrogen atoms, is coordinated via hydrogen water atoms. The N-C bond lengths in HMTA range from 1.471 to 1.481 Å, and the N-C-N angles range from 111.53° to 112.12°. which is close to ideal tetrahedral angles. The bromide anion interacts with the aqua cation [Ni(H₂O)₆]²⁺ through the hydrogen atoms of crystallized water, forming complex hydrogen bonds.

X-ray diffraction analysis further identified a network of intermolecular hydrogen bonds, including O-H...O, O-H...H, C-H...O, and Br...H-O interactions, which play a crucial role in the stabilization of the crystal lattice. These interactions form a three-dimensional hydrogen-bonded framework that enhances the stability of the coordination complex.

Thermal analysis demonstrated that $NiBr_2 \times 2(CH_2)_6N_4 \times 10H_2O$ remains stable up to 150°C, with the first decomposition stage corresponding to dehydration. The second decomposition stage, observed at ~200°C, involves the breakdown of hexamethylenetetramine, followed by the complete structural collapse at temperatures above 300°C. Differential scanning calorimetry confirmed

distinct endothermic transitions associated with each decomposition step, corroborating thermogravimetric analysis data.

Infrared spectroscopy validated the structural findings by identifying characteristic vibrational bands: Ni-O stretching (450-600 cm⁻¹), N-C vibrations from HMTA (1300–1600 cm⁻¹), and O-H stretching associated with hydrogen bonding interactions (3200-3600 cm⁻¹). These results confirm the role of hydrogen bonding in maintaining the stability of the complex.

Overall, this study provides a comprehensive structural and thermal characterization of NiBr₂×2(CH₂)₆N₄× ×10H₂O, highlighting its stability, coordination behavior, and hydrogen bonding interactions. These findings contribute to the understanding of coordination chemistry and offer insights into potential applications in materials science and catalysis.

References

- Ishak, N. N. M.; Jamsari, J.; Ismail, A. Z.; Tahir, M. I. M.; Tiekink, E. R. T.; Veerakumarasivam, A.; Ravoof, T. B. S. A. Synthesis, Characterisation and Biological Studies of Mixed-Ligand Nickel (II) Complexes Containing Imidazole Derivatives and Thiosemicarbazide Schiff Bases. J. Mol. Struct. 2019, 119815, 126888. https://doi.org/10.1016/j.molstruc.2019.126888 Ou, G.: Wang, O.: Tan, Y.: Zhou, O. Synthesis, Structures, and Magnetism of Four One-Dimensional Complexes Using [Ni(CN)4]2- and Macrocyclic Metal Complexes. Molecules 2023, 28, 4529. https://doi.org/10.3390/molecules28114529 Alramadhan, S. A.; Hammud, H. H.; Ali, B. F.; Ghabbour, H. A.; Sarfaraz, S.; Ayub, K. Structures, Characterization and DFT Studies of Four Novel Nickel Phenanthroline Complexes. Crystals 2023, 13, 738. https://doi.org/10.3390/cryst13050738 [4] Graf, M.; Ochs, J.; Mayer, P.; Metzler-Nolte, N.; Böttcher, H.-C. Cytotoxic Activity of Some Half-Sandwich Rhodium(III) Complexes Containing 4,4'-Disubstituted-2,2'-bipyridine Ligands. Z. Anorg. Allg. Chem. 2024, 650, e202300195. https://doi.org/10.1002/zaac.202300195 Teng, O.; Huynh, H. V. A Unified Ligand Electronic Parameter Based on 13C NMR Spectroscopy of N-Heterocyclic Carbene Complexes. *Dalton Trans.* **2017**, *46*, 614–627. https://doi.org/10.1039/C6DT04222H Opalade, A. A.; Labadi, I.; Gomez-Garcia, C.; Hietsoi, O.;
- Gerasimchuk, N. Nickel(II) Aqua Complexes with Chelating Ligands: What Happens When Water Is Gone? Cryst. Growth Des. 2022, 22, 6168-6182.

https://doi.org/10.1021/acs.cgd.2c00717

- Hazra, S.; Das, L. K.; Bhattacharya, R.; Drew, M. G. B.; Ghosh, A. Variations of Structures on Changing the Ratios of Metal Ions in Rare Ca(II)-Zn(II) Hetero-Metallic Self-Assembled Coordination Polymers of Hexamethylenetetramine and Benzoate. J. Indian Chem. Soc. 2021, 98, 100097.
- https://doi.org/10.1016/j.jics.2021.100097
- Martí Valls, R.; García Rodríguez, R.; Meza Rojas, D.; Dunlop, T.; Jones, E.; Thomas, S. K.; Davies, M. L.; Holliman, P. J.; Baker, J.; Charbonneau, C. A Facile Method to Obtain Colloidal Dispersions of Nickel Hydroxide: Improving the Processing of Nickel Oxide and Facilitating its Upscaling for
- 423 Perovskite-Type Solar Devices. Colloids Surf., A 2024, 6985, 134524. https://doi.org/10.1016/j.colsurfa.2024.134524 [9] Shahadat, H. M.; Ahmad, N.; Khattak, Z. A. K.; Abdur, R. M.; Al-Hajri, R.; Al-Abri, M.; Kao, C.-M.; Younus, H. A.; Verpoort, F. Highly Active Macrocyclic Nickel(II) complex for Hydrogen Evolution Reaction in Neutral Aqueous Conditions. Int. J. Hydrogen Energy 2023, 48, 33927–3393629. https://doi.org/10.1016/j.ijhydene.2023.05.192 [10] Wang, Y.; Wang, Y.; Huang, X.; Chen, M.; Xu, Y. Ni(NH3)62+ More Efficient than Ni(H2O)62+ and Ni(OH)2 for Catalyzing Water and Phenol Oxidation on Illuminated Bi2MoO6 with Visible Light. J. Environ. Sci. 2022, 126, 556-564. https://doi.org/10.1016/j.jes.2022.05.021 [11] Manimaran, P.; Balasubramaniyan, S.; Azam, M.; Rajadurai, D.; Al-Resayes, S. I.; Mathubala, G.; Manikandan, A.; Muthupandi, S.; Tabassum, Z.; Khan, I. Synthesis, Spectral Characterization and Biological Activities of Co(II) and Ni(II) Mixed Ligand Complexes. Molecules 2021, 26, 823. https://doi.org/10.3390/molecules26040823 [12] Dinzhos, R. V.; Privalko, E. G.; Privalko, V. P. Enthalpy Relaxation in the Cooling/Heating Cycles of Polyamide 6/Organoclav Nanocomposites, I. Nonisothermal Crystallization. J. Macromol. Sci. Part B Phys. 2005, 44, 421-430. https://doi.org/10.1081/MB-200061610 [13] Privalko, V. P.; Dinzhos, R. V.; Privalko, E. G. Melting Behavior of the Nonisothermally Crystallized Polypropylene/Organosilica Nanocomposite. J. Macromol. Sci. Part B Phys. 2004, 43, 979-988. https://doi.org/10.1081/MB-200033272 [14] Li, Y. J.; Guo, S. Z.; Feng, T.; Xie, K. F.; Dong, W. K. An Investigation into Three-Dimensional Octahedral Multi-Nuclear Ni(II)-Based Complexes Supported by a More Flexible Salamo-Type Ligand. J. Mol. Struct. **2021**, 1228, 129796. https://doi.org/10.1016/j.molstruc.2020.129796 [15] Barzegar Kiadehi, S.; Golchoubian, H. Synthesis, Characterization, Hirshfeld Surface Analysis, and Chromotropic Behavior of a Novel Copper(II) Complex with Amide-Pyridyl Ligand: Solvato-, Halo-, and thermochromism and Azide Ion Sensing. Struct. Chem. 2025, 36, 469-482. https://doi.org/10.1007/s11224-024-02384-4 [16] Kargar, H.; Ashfaq, M.; Fallah-Mehrjardi, M.; Behjatmanesh-Ardakani, R.; Munawar, K. S.; Tahir, M. N. Synthesis, Crystal Structure, Spectral Characterization, Theoretical and Computational Studies of Ni(II), Cu(II) and Zn(II) Complexes Incorporating Schiff Base Ligand Derived from 4-(Diethylamino)salicylaldehyde. Inorg. Chim. Acta 2022, 536, 120878. https://doi.org/10.1016/j.ica.2022.120878 [17] Kargar, H.; Ardakani, A. A.; Tahir, M. N.; Ashfaq, M.; Munawar, K. S. Synthesis, Spectral Characterization, Crystal Structure and Antibacterial Activity of Nickel(II), Copper(II) and Zinc(II) Complexes Containing ONNO Donor Schiff Base Ligands. J. Mol. Struct. 2021, 1233, 130112. https://doi.org/10.1016/j.molstruc.2021.130112 [18] Zhang, X.; Zhang, J.; Hao, Z.; Han, Z.; Lin, J.; Lu, G. L. Nickel Complexes Bearing N.N.O-Tridentate Salicylaldiminato Ligand: Efficient Catalysts for Imines Formation via

Dehydrogenative Coupling of Primary Alcohols with Amines.

[19] Nemoshkalenko, V. V.; Borisenko, S. V.; Uvarov, V. N.;

Yaresko, A. N.; Vakhney, A. G.; Senkevich, A. I.; Borisenko, T.

N.; Borisenko, V. D. Electronic structure of the R₂Ti₂O₇ (R =Sm-

Organometallics 2021, 40, 3843-3853.

https://doi.org/10.1021/acs.organomet.1c00552

424 Er, Yb, Lu) oxides. Phys. Rev. B 2001, 63, 075106. https://doi.org/10.1103/PhysRevB.63.075106 [20] Kunitskii, Y.A., Bespalov, Y.A., Korzhik, V.N. Structural heterogeneities in amorphous materials from a Ni-Nb alloy. Powder Metall Met Ceram 1988, 27, 763-767. https://doi.org/10.1007/BF00802767 [21] Zhurakovsky, Y. A.; Korzhik, V. N.; Borisov, Y. S. Finestructure of roentgen emission-spectra of alloy Ni-Nb in amorphous and crystalline states. Izvest. Vyssh. Ucheb. Zaved. Fiz. **1988**, 31, 108-110. [22] Dey, P.; Islam, S.; Seth, S. K. Quantitative Analysis of the Interplay of Hydrogen Bonds in M(II)-Hexaaqua Complexes with HMTA [M(II)=Co(II), Mg(II); HMTA=Hexamethylenetetramine]. J. Mol. Struct. 2023, 1284, 135448. https://doi.org/10.1016/j.molstruc.2023.135448 [23] Inada, Y.; Mohammed, A. M.; Loeffler, H. H.; Rode, B. M. Hydration Structure and Water Exchange Reaction of Nickel(II) Ion: Classical and QM/MM Simulations. J. Phys. Chem. A 2002, 106, 6783-6791. https://doi.org/10.1021/jp0155314 [24] Asemave, K.; Buluku, G. T.; Abah, C. N.; Ngise, T. H. Determination of Binary Stability Constant of the Complexes of Ni(II) and Mn(II) Ions with Cysteine. ChemSearch J. 2023, 14, 84-89. [25] Kuznetsov, B. N.; Chesnokov, N. V.; Mikova, N. M.; Zaikovskii, V. I.; Drozdov, V. A.; Savos'kin, M. V.; Yaroshenko, A. M.; Lyubchik, S. B. Texture and catalytic properties of palladium supported on thermally expanded natural graphite. React. Kinet. Catal. Let. 2003, 80, 345-350. https://doi.org/10.1023/B:REAC.0000006144.22936.ac [26] Li, L. L.; Feng, S. S.; Zhang, T.; Wang, L.; Don, W. K. Counteranion-Solvent-Dependent Ni(II)-Based Complexes with π - π Interactions: Synthesis, Crystal Structure and Catalytic Properties. Polyhedron 2019, 170, 715-720. https://doi.org/10.1016/j.poly.2019.06.043 [27] Zhang, J.-W.; Liu, W.-H.; Wang, C.-R.; Xu, S.; Liu, B.-Q.; Dong, Y.-P. Syntheses and Properties of Three Types of 3,4-Dichlorobenzoate-based Ni(II)-Ln(III) Heterometallic Clusters. ChemistrySelect. 2019, 4, 12418-12423. https://doi.org/10.1002/slct.201902628 [28] Mehmeti, B.; Kelmendi, J.; Iiljazi-Shahiqi, D.; Azizi, B.; Jakovljevic, S.; Haliti, F.; Anic-Milosevic, S. Comparison of Shear Bond Strength Orthodontic Brackets Bonded to Zirconia and Lithium Disilicate Crowns. Acta Stomatol. Croat. 2019, 53, 17-27. https://doi.org/10.15644/asc53/1/2 [29] Ushenko, Y. A.; Dubolazov, A. V.; Angelsky, A. P.; Sidor, M. I.; Bodnar, G. B.; Koval, G.; Zabolotna, N. I.; Smolarz, A.; Junisbekov, M. S. Laser polarization fluorescence of the networks of optically anisotropic biological crystals. Proceed. SPIE - Int. Soc. Optic. Engin. 2013, 8698, 869809. https://doi.org/10.1117/12.2019350 [30] Takahashi, K.; Nakamura, T.; Akutagawa, T. Dynamic Supramolecular Cations in Conductive and Magnetic [Ni(dmit)2] Crystals. Coord. Chem. Rev. 2023, 475, 214881. https://doi.org/10.1016/j.ccr.2022.214881

[31] Li, J. X.; Zhang, Y. H.; Du, Z. X.; Feng, X. One-Pot

120697. https://doi.org/10.1016/j.ica.2021.120697

Solvothermal Synthesis of Mononuclear and Oxalate-Bridged

[32] Newman-Stonebraker, S. H.; Raab, T. J.; Roshandel, H.;

Oxidation and Ligand Displacement: Evaluation of Ligand Effects

Doyle, A. G. Synthesis of Nickel(I)-Bromide Complexes via

Binuclear Nickel Compounds: Structural Analyses, Conformation Alteration, and Magnetic Properties. *Inorg. Chim. Acta* **2021**, *530*,

on Speciation and Reactivity. J. Am. Chem. Soc. 2023, 145, 19368-19377. https://doi.org/10.1021/jacs.3c06233 [33] Liu, R.; Liu, Y.; Yang, W.; Li, X.; Feng, L. Chromiumbased Complexes Bearing Aminophosphine and Phosphine-Imine-Pyrryl Ligands for Selective Ethylene tri/Tetramerization. ACS Omega 2023, 8, 18290-18298. https://doi.org/10.1021/acsomega.3c02083 [34] Pérez-Bitrián, A.; Hoffmann, K. F.; Krause, K. B.; Thiele, G.; Limberg, C.; Riedel, S. Unravelling the Role of the Pentafluoroorthotellurate Group as a Ligand in Nickel Chemistry. Chem. Eur. J. 2022, 28, e202202016. https://doi.org/10.1002/chem.202202016 [35] Sakthivel, R. V.; Sankudevan, P.; Vennila, P.; Venkatesh, G.; Kaya, S.; Serdaroğlu, G. Experimental and Theoretical Analysis of Molecular Structure, Vibrational Spectra and Biological Properties of the New Co(II), Ni(II) and Cu(II) Schiff Base Metal Complexes. J. Mol. Struct. 2021, 1233, 130097. https://doi.org/10.1016/j.molstruc.2021.130097 [36] Stasevych, M.; Zvarych, V.; Dronik, M.; Sozanskyi, M.; Khomyak, S. Application of Infrared Spectroscopy and X-ray Powder Diffractometry for Assessment of the Qualitative Composition of Components in a Pharmaceutical Formulation. Chem. Chem. Technol. 2023, 17, 510-517. https://doi.org/10.23939/chcht17.03.510 [37] Hrynyshyn, K.; Skorokhoda, V.; Chervinskyy, T. Study on the Composition and Properties of Pyrolysis Pyrocondensate of Used Tires. Chem. Chem. Technol. 2022, 16, 159-163. https://doi.org/10.23939/chcht16.01.159

Received: November 04, 2024 / Revised: February 06, 2025 / Accepted: March 12, 2025

СТРУКТУРНО-КООРДИНАЦІЙНІ ОСОБЛИВОСТІ ГІДРАТОВАНОЇ КОМПЛЕКСНОЇ СПОЛУКИ НІКЕЛЬ БРОМІДУ З ГЕКСАМЕТИЛЕНТЕТРАМІНОМ

Анотація. Комплексну сполуку $NiBr_2 \times 2(CH_2)_6 N_4 \times$ $\times 10H_2O$ було синтезована та структурно охарактеризовано за допомогою рентгенівської кристалографії, термогравіметричного аналізу, диференційної сканувальної калориметрії й інфрачервоної спектроскопії. Комплекс кристалізується в моноклінній системі (Р21/с) з октаедричним координаційним оточенням нікелю, де довжини зв'язків Ni-O варіюються в межах 2.027-2.058 Å. Термогравіметричний аналіз підтвердив стабільність сполуки до 150°С, після чого відбувається дегідратація, розкладання ГМТА за 200°С і руйнування координаційного каркасу вище 300°С. ДСК виявила чітко виражені ендотермічні переходи. У спектрах ІЧ-спектроскопії виявлено смуги розтягувальних коливань Ni-O (450-600 см⁻¹), N-C (1300- 1600 см^{-1}) та O-H (3200–3600 см $^{-1}$), що підтверджує наявність водневих зв'язків. Отримані результати дають кількісне уявлення про структурну стабільність, термічну поведінку та систему водневих зв'язків цієї сполуки, що може знайти застосування в матеріалознавстві та каталізі.

Ключові слова: полідентатний ліганд, внутрішньомолекулярні взаємодії, міжатомні відстані, координаційна хімія, водневі зв'язки, термодинамічні параметри.